Analysis of PHA-1 Reveals a Limited Role in Pharyngeal Development and Novel Functions in Other Tissues

Aleksandra Kuzmanov,[1] John Yochem,[1] and David S. Fay[2]
Department of Molecular Biology, College of Agriculture and Natural Resources, University of Wyoming, Laramie, Wyoming 82071

ABSTRACT PHA-1 encodes a cytoplasmic protein that is required for embryonic morphogenesis and attachment of the foregut (pharynx) to the mouth (buccal capsule). Previous reports have in some cases suggested that PHA-1 is essential for the differentiation of most or all pharyngeal cell types. By performing mosaic analysis with a recently acquired *pha-1* null mutation (*tm3671*), we found that PHA-1 is not required within most or all pharyngeal cells for their proper specification, differentiation, or function. Rather, our evidence suggests that PHA-1 acts in the arcade or anterior epithelial cells of the pharynx to promote attachment of the pharynx to the future buccal capsule. In addition, PHA-1 appears to be required in the epidermis for embryonic morphogenesis, in the excretory system for osmoregulation, and in the somatic gonad for normal ovulation and fertility. PHA-1 activity is also required within at least a subset of intestinal cells for viability. To better understand the role of PHA-1 in the epidermis, we analyzed several apical junction markers in *pha-1(tm3671)* homozygous embryos. PHA-1 regulates the expression of several components of two apical junction complexes including AJM-1–DLG-1/discs large complex and the classical cadherin–catenin complex, which may account for the role of PHA-1 in embryonic morphogenesis.

MUTATIONS in the *pha-1* locus were first described ~25 years ago (Schnabel and Schnabel 1990; Granato *et al.* 1994a). Recessive *pha-1* loss-of-function (LOF) mutations confer arrest as embryos or L1-stage larvae that display gross defects in pharyngeal development and body morphogenesis. Subsequent studies have shown that PHA-1 is part of a regulatory network that includes two Zn-finger proteins, SUP-35/ZTF-21 and SUP-37/ZTF-12, and a Skp1-related protein, SUP-36 (Schnabel *et al.* 1991; Mani and Fay 2009; Fay *et al.* 2012; Polley *et al.* 2014). Genetically, SUP-35–37 act at the same step, possibly within the context of a multiprotein complex (Polley *et al.* 2014). Notably, LOF mutations in *sup-35*, *sup-36*, or *sup-37* completely suppress the lethality of *pha-1* null and partial-LOF mutations, and overexpression of SUP-35 and SUP-36 can phenocopy *pha-1* LOF (Mani and Fay 2009; Fay *et al.* 2012; Polley *et al.* 2014). These observations have led to the model that SUP-35–37 function in a manner that opposes or is antagonistic to PHA-1. Other regulators of this network include LIN-35, the *Caenorhabditis elegans* retinoblastoma protein (pRb) ortholog, and HCF-1, an ortholog of human host cell factor 1 (HCF1) (Fay *et al.* 2004; Mani and Fay 2009). LIN-35 and HCF-1 are positive and negative regulators of *sup-35* transcription, respectively. In addition, both SUP-35 and SUP-36 are negatively regulated post-translationally by a conserved E2–E3 complex composed of UBC-18/UBCH7 and ARI-1/HHARI, which promotes ubiquitin-mediated proteolysis (Qiu and Fay 2006; Mani and Fay 2009; Fay *et al.* 2003, 2012; Polley *et al.* 2014).

pha-1 encodes a novel cytoplasmic protein that contains a DUF1114 domain of unknown function (Granato *et al.* 1994a; Fay *et al.* 2004). Although multiple PHA-1-related proteins are present in *C. elegans* and several closely related species (*i.e.*, members of the *elegans* and *Japonica* super groups), orthologs of PHA-1 are not detected in most nematodes or in other metazoa. Notably, *pha-1* is among the small minority (~15%) of *C. elegans* genes whose functions are required for viability under laboratory conditions (Schnabel and Schnabel 1990; Kemphues 2005). Thus,

doi: 10.1534/genetics.114.166876
Manuscript received June 3, 2014; accepted for publication June 30, 2014; published Early Online July 9, 2014.
Available freely online through the author-supported open access option.
Supporting information is available online at http://www.genetics.org/lookup/suppl/doi:10.1534/genetics.114.166876/-/DC1.
[1]These authors contributed equally to this work.
[2]Corresponding author: Department of Molecular Biology, College of Agriculture and Natural Resources, Department 3944, 1000 E. University Ave., University of Wyoming, Laramie, WY 82071. E-mail: davidfay@uwyo.edu

pha-1 is quite unusual in that it is not highly conserved but is nevertheless an essential gene. Moreover, our understanding of the molecular, cellular, and developmental functions of PHA-1 has remained elusive.

Although the importance of PHA-1 during embryonic development is clear, previous reports regarding the specific functions of PHA-1 during development have led to conflicting conclusions. In particular, the role of PHA-1 in pharyngeal cell differentiation is unclear (Schnabel and Schnabel 1990; Granato *et al.* 1994b; Okkema *et al.* 1997; Fay *et al.* 2004). Surprisingly, we found that the role of PHA-1 in pharyngeal development appears to be restricted to a small subset of cells and that PHA-1 does not appear to have a direct or essential role in pharyngeal cell specification or differentiation. Moreover, we provide evidence that PHA-1 carries out functions in several tissues not previously known to require PHA-1 activity, including an essential role in the intestine. This latter finding is consistent with our previous work showing that *pha-1* is ubiquitously expressed in embryos, larvae, and adults (Fay *et al.* 2004). Our analysis further indicates that PHA-1 influences the expression or localization of several apical junction proteins, which may account for its function in epithelial morphogenesis and possibly other cell types during development.

Materials and Methods

Strains and maintenance

C. elegans strains were maintained according to standard methods (Stiernagle 2006). Strains used in this study include GE24 [*pha-1(e2123) III*], WY847 [*pha-1(tm3671) III*; *fdEx181* (pBX (*pha-1*–wild-type genomic locus); *sur-5*::*GFP*)], WY848 [*pha-1(tm3671) III*; *fdEx182* (pBX; *sur-5*::*GFP*)], WY849 [*pha-1(tm3671) III*; *fdEx183* (pBX; *sur-5*::*GFP*)], MH1384 [*kuIs46* (AJM-1::*GFP*; *unc-119*+ *X*)], MH1385 [*kuIs47* (AJM-1::*GFP*; *unc-119*+ *II*)], WY924 [*pha-1(tm3671) III*; *kuIs47 II*; *fdEx182*], WY876 [*pha-1(tm3671) III*, *kuIs46 X*; *fdEx182*], SU159 [*ajm-1(ok160)*; *jcEx44(*AJM-1::*GFP)*], SM481 [*Is* ($P_{pha\text{-}4}$::*GFP*-mem + pRF4)], WY871 [*pha-1(tm3671) III*, *Is* ($P_{pha\text{-}4}$::*GFP*-mem + pRF4); *fdEx182*], WY872 [*pha-1(e2123) III*, Is ($P_{pha\text{-}4}$::GFP-mem + pRF4); *fdEx182*], SU295 [*jcIs25* (*pPE103* (JAC-1::GFP); pRF4)] (Pettitt *et al.* 2003), WY997 [*pha-1(tm3671) III*; *jcIs25*; *fdEx182*], FT250 [*unc-119(ed3) III*; *xnIs96* (*pJN455* (HMR-1::GFP) + *unc-119*+] (Achilleos *et al.* 2010), WY996 [*pha-1(tm3671) III*; *xnIs96*; *fdEx182*], TH502 [*unc-119(ed3) III*; *ddIs290* (SAX-7::GFP + *unc-119*+)] (Sarov *et al.* 2012), WY995 [*pha-1(tm3671) III*; *ddIs290*; *fdEx182*], SU265 [*jcIs17* (HMP-1::GFP + DLG-1::dsRed + pRF4)] (Raich *et al.* 1999), and WY990 [*pha-1(tm3671) III*; *jcIs17*; *fdEx182*].

Mosaic analysis

Mosaic analysis was carried out using strains WY847, WY848, and WY849 following established protocols (Yochem *et al.* 2000; Yochem 2006).

Microscopy

GFP and dsRed fluorescence images were collected using a Nikon Eclipse epifluorescence microscope and OpenLab software, and quantification was carried out using ImageJ. Averages of the mean fluorescence of the entire embryo were calculated to compare expression levels and backgrounds were subtracted using identically sized areas from an empty region of the slide. Fluorescence intensities provided in the figures are in arbitrary units. *P*-values were determined using a two-tailed Student's *t*-test.

Results

PHA-1 is required for pharyngeal cell reorientation and the stable attachment of arcade cells to pharyngeal epithelial cells

The *C. elegans* pharynx (foregut) is an organ derived from 95 primordial cells that differentiate into seven distinct cell types (arcade, epithelial, muscle, gland, marginal, valve, and neural) (Albertson and Thomson 1976; Mango 2007, 2009). A principal function of the pharynx is to ingest food, to mechanically process it, and to deposit it into the intestine. Studies of pharyngeal morphogenesis by Portereiko and Mango (2001) defined three temporally separated steps (Figure 1, A and B). In the first step, termed reorientation, anterior pharyngeal epithelial cells are converted from a radial configuration into two parallel rows through changes in cell shape, location, and apicobasal polarity. In the second step, termed epithelialization, reorientated pharyngeal cells attach to the neighboring arcade cells, which are anterior to the pharynx, to form a contiguous epithelial tube connecting the nascent buccal cavity (mouth) to the intestine. In the third step, termed contraction, localized forces pull the arcade and pharyngeal epithelial cells closer together, and the pharynx shifts *en masse* slightly toward the anterior. This initiates the conversion of the primordial pharynx from a ball of cells into an elongated bilobed tube connecting the mouth to the intestine (Figures 1, B and C). Notably, the first step, reorientation, is essential for all subsequent steps of morphogenesis to occur.

Previous phenotypic analyses of *pha-1* employed what are now known to be partial-LOF alleles (*e.g.*, *pha-1(e2123)* (referred to as *pha-1(ts)*), which may differ from the phenotypes displayed by null mutants (Schnabel and Schnabel 1990; Granato *et al.* 1994a; Fay *et al.* 2004; Mani and Fay 2009). We therefore examined pharyngeal morphogenesis using strains homozygous for the *pha-1(tm3671)* (*pha-1(0)*) null deletion, which contain a 203-bp deletion that removes the N-terminal portion of the second *pha-1* exon and creates a premature stop codon (Fay *et al.* 2012). Cell-shape changes during pharyngeal morphogenesis were visualized using a *pha-4*-driven plasma membrane–GFP reporter that is expressed exclusively within cells of the pharyngeal primordium, intestine, and arcade cells (Portereiko and Mango 2001; Fay *et al.* 2003).

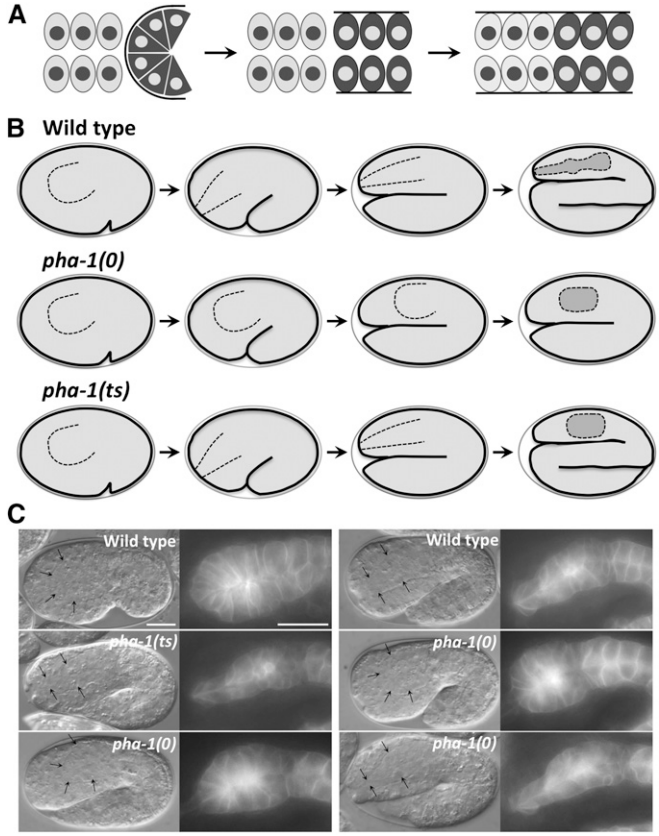

Figure 1 Pharyngeal morphogenesis in wild-type and *pha-1* mutants. (A) Schematic diagram of early stages of pharyngeal morphogenesis (after Portereiko and Mango 2001) showing the initial state, reorientation, and epithelialization/contraction (left to right). Arcade cells are indicated in light shading, pharyngeal cells in dark shading. Thick solid lines indicate the locations of basement membranes. (B) Overview of pharyngeal morphogenesis during embryogenesis in wild type and *pha-1* mutants. Note differences between the phenotypes of *pha-1(0)* and *pha-1(ts)* mutants. Also note that *pha-1(0)* mutants fail to progress beyond the twofold stage of embryogenesis. Dashed lines indicate pharyngeal boundaries. (C) Representative images of P_{pha-4}::membrane–GFP reporter expression in wild-type, *pha-1(ts)* at 25°, and *pha-1(0)* embryos. Anterior is to the left, dorsal is up. Corresponding DIC (left) and fluorescence images (right) are paired for each embryo. Bars in wild-type DIC and fluorescence images, 10 μm for DIC and fluorescence images, respectively. Solid arrows indicate the anterior border of the developing pharynx. Note that both wild type (50/50) and *pha-1(ts)* mutants at 25° (47/48) show extension by the 1.5-fold stage. In contrast, the large majority of *pha-1(0)* embryos do not undergo any obvious extension (38/44). Furthermore, in *pha-1(0)* mutants that did undergo pharyngeal extension (lower right paired panels), the width of the pharynx was often narrower along the dorsal–ventral axis than in wild type.

Consistent with our previous observations (Fay *et al.* 2004), a large majority of *pha-1(ts)* mutants (47/48) incubated at the nonpermissive temperature of 25° were capable of completing reorientation, initiating attachment to the arcade cells, and establishing a transient connection to the nascent buccal cavity (Figure 1, B and C). In contrast, the large majority of *pha-1(0)* embryos (38/44) did not undergo reorientation and failed to integrate with the arcade cells (Figure 1, B and C). Furthermore, in *pha-1(0)* mutants that did undergo reorientation, the developing anterior pharynx was often abnormally constricted along the dorsal–ventral axis (Figure 1C). A role for PHA-1 in reorientation is also consistent with reorientation defects observed in *lin-35*; *pha-1(fd1)* and *lin-35*; *ubc-18* double mutants (Fay *et al.* 2003, 2004). We also note that equivalent levels of expression of the P_{pha-4}::membrane–GFP reporter in wild type, *pha-1(ts)* and *pha-1(0)* mutants indicates that a reduction or loss of PHA-1 activity does not affect the specification of the pharyngeal primordium (Figure 1).

The highly penetrant pharynx unattached (Pun) phenotype of *pha-1(ts)* mutants indicates that PHA-1 is also required for the maintenance of pharyngeal attachment to the buccal capsule at later stages of development. Furthermore, on the basis of the arcade cell marker, *bath-15*::*GFP* (Shaw *et al.* 2010), we found that the buccal capsule in *pha-1(ts)* mutants is typically severed or discontinuous, with the break occurring at the junction of the arcade and pharyngeal epithelial cells (Supporting Information, Figure S1). In more subtle cases, a morphologically abnormal X-shaped (Chi) structure was detected at the junction of the arcade and pharyngeal cells (Figure S1), which may interfere with the ability of these animals to feed, thereby leading to larval arrest. Taken together, our findings demonstrate that PHA-1 is critical for both the initiation and maintenance of pharyngeal epithelial cell attachment to the arcade cells.

Several epithelial apical junction markers are misregulated in pha-1 mutants

To further characterize pharyngeal defects in *pha-1(0)* mutants, we made use of a fluorescence reporter for AJM-1, an apical junction protein that is broadly required for morphogenesis and the integrity of epithelia in *C. elegans* (Koppen *et al.* 2001; McMahon *et al.* 2001; Lynch and Hardin 2009). For these assays, AJM-1::GFP served as a marker of epithelialization for both the pharynx and arcade cells (Portereiko and Mango 2001). Consistent with previous reports, AJM-1::GFP is first detected in wild-type embryos beginning at the lima-bean stage (~350 min postfertilization) in the central region of the primordial pharynx (Figure 2). Expression of AJM-1::GFP is also observed in the region corresponding to the arcade cells beginning at around the comma stage (~400 min), coincident with the onset of reorientation. Expression of AJM-1::GFP increases throughout the 1.5- and 2.0-fold stages of embryogenesis in both the pharynx and arcade regions of wild-type embryos (~430–450 min; Figure 2).

Although *pha-1(ts)* mutants at 25° displayed a similar pattern of AJM-1::GFP to that of wild-type embryos, expression was typically weaker and less uniform than expression in wild type at corresponding stages (Figure 2). In contrast, AJM-1::GFP expression was dramatically reduced in *pha-1(0)* mutants with little or no detectable expression in the region of the primordial pharynx through the 2.0-fold stage (Figure 2). In addition, *pha-1(0)* mutants that failed to undergo reorientation never expressed AJM-1::GFP in the region of the arcade cells, consistent with the model that epithelialization of the

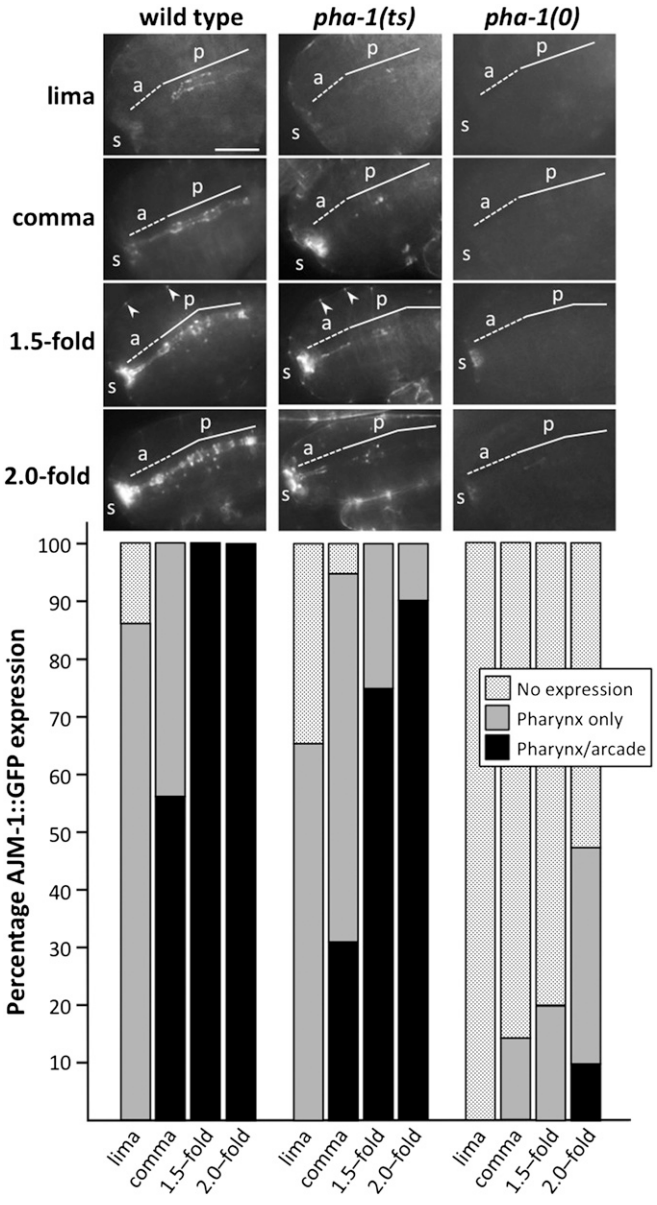

Figure 2 AJM-1::GFP expression in *pha-1* mutants. Representative images of AJM-1::GFP (*kuIs46*) in wild-type, *pha-1(ts)* at 25°, and *pha-1 (0)* embryos at the indicated stages. Anterior is to the left, dorsal is up. Location of the pharynx (p) is indicated with a solid white line, and arcade cells (a) are indicated with a dashed white line (sensory depression, s). Arrowheads indicate AJM-1 puncta in the developing epidermis. Bar, 5 μm. Graph shows quantification of AJM-1::GFP expression patterns for each genotype and stage. The number of embryos examined for each stage and genotype ranged from 21 to 32.

arcade cells strictly follows integration with the anterior pharynx (Portereiko and Mango 2001). Although some 2.0-fold *pha-1(0)* embryos did not express AJM-1::GFP, expression was always observed in late-stage, terminally arrested *pha-1(0)* embryos, although levels were strongly reduced as compared with wild type (Figure S2). Similar results were also observed using an independent array of AJM-1::GFP integrated on a different chromosome (data not shown). Finally, AJM-1::GFP expression defects in *pha-1(0)* mutants were fully rescued by an extrachromosomal array containing wild-type copies of *pha-1* or by inhibition of *sup-35* by RNAi (Figure S2). These findings indicate that PHA-1 plays an important role in the timing and strength of AJM-1 expression and more generally in the process of pharyngeal epithelialization. They also demonstrated that suppression and rescue of *pha-1(0)* defects correlates with the normal expression of AJM-1.

In our studies examining the expression of AJM-1::GFP in the embryonic pharynx, we noticed that this marker was expressed at much lower levels in the developing embryonic epidermis (formerly termed the hypodermis) of *pha-1(0)* null mutants as compared with wild-type or *pha-1(ts)* embryos (Figure 2 and Figure 3B). To see if our observation was specific to AJM-1 or reflected a more generalized defect in the epithelia of *pha-1(0)* mutants, we examined expression patterns of several markers associated with adherens junctions and integrity in 1.5-fold *pha-1(0)* embryos. Two well-characterized junctional complexes in *C. elegans* include a classical cadherin–catenin complex (HMR-1/cadherin, JAC-1/p120-catenin, HMP-1/α-catenin and HMP-2/β-catenin) and the more basal AJM-1 and DLG-1/discs large complex (Labouesse 2006; Lynch and Hardin 2009). DLG-1, a binding partner of AJM-1, is essential for proper localization of AJM-1 (Koppen *et al.* 2001), whereas SAX-7 has been proposed to function as the transmembrane component of the complex (Chen *et al.* 2001). Loss of *pha-1* resulted in a strong reduction in AJM-1::GFP in the pharynx and intestine (4.6-fold), and lateral epithelial cells (5.4-fold; Figure 3B). In addition, a modest increase in DLG-1::dsRed expression (1.5- to 1.7-fold) was observed in both the epidermis and gastrointestinal tract of *pha-1(0)* mutants, whereas no obvious changes were detected with SAX-7::GFP (Figure 3B). In the case of the cadherin–catenin complex, expression of HMR-1::GFP was reduced ~1.9-fold in both the pharynx and epidermis of *pha-1(0)* mutants, whereas JAC-1 expression was enhanced 1.4- to 1.6-fold in the pharynx and epidermis (Figure 3C). In contrast, HMP-1::GFP showed no change in *pha-1(0)* mutants (Figure 3C). Our results indicate that components of two major junctional complexes are misregulated in epithelial cells of *pha-1(0)* mutants, consistent with the role of PHA-1 in regulating epidermal morphogenesis.

PHA-1 is not required autonomously for the differentiation or function of most pharyngeal cells

To better understand the role of PHA-1 in pharyngeal development and to more broadly identify tissues in which PHA-1 performs important functions, we carried out a mosaic analysis using the *pha-1(0)* allele strain. These strains have a mitotically unstable extrachromosomal array containing wild-type *pha-1* [*pha-1(+)*] rescuing sequences along with a broadly expressed visible marker, SUR-5::GFP (Yochem *et al.* 1998). These strains produce animals containing a mixture of wild-type and *pha-1(0)* mutant cells that can be distinguishable by the presence or absence of nuclear GFP. The pattern of array inheritance was used to determine the cell lineages in which the array was retained

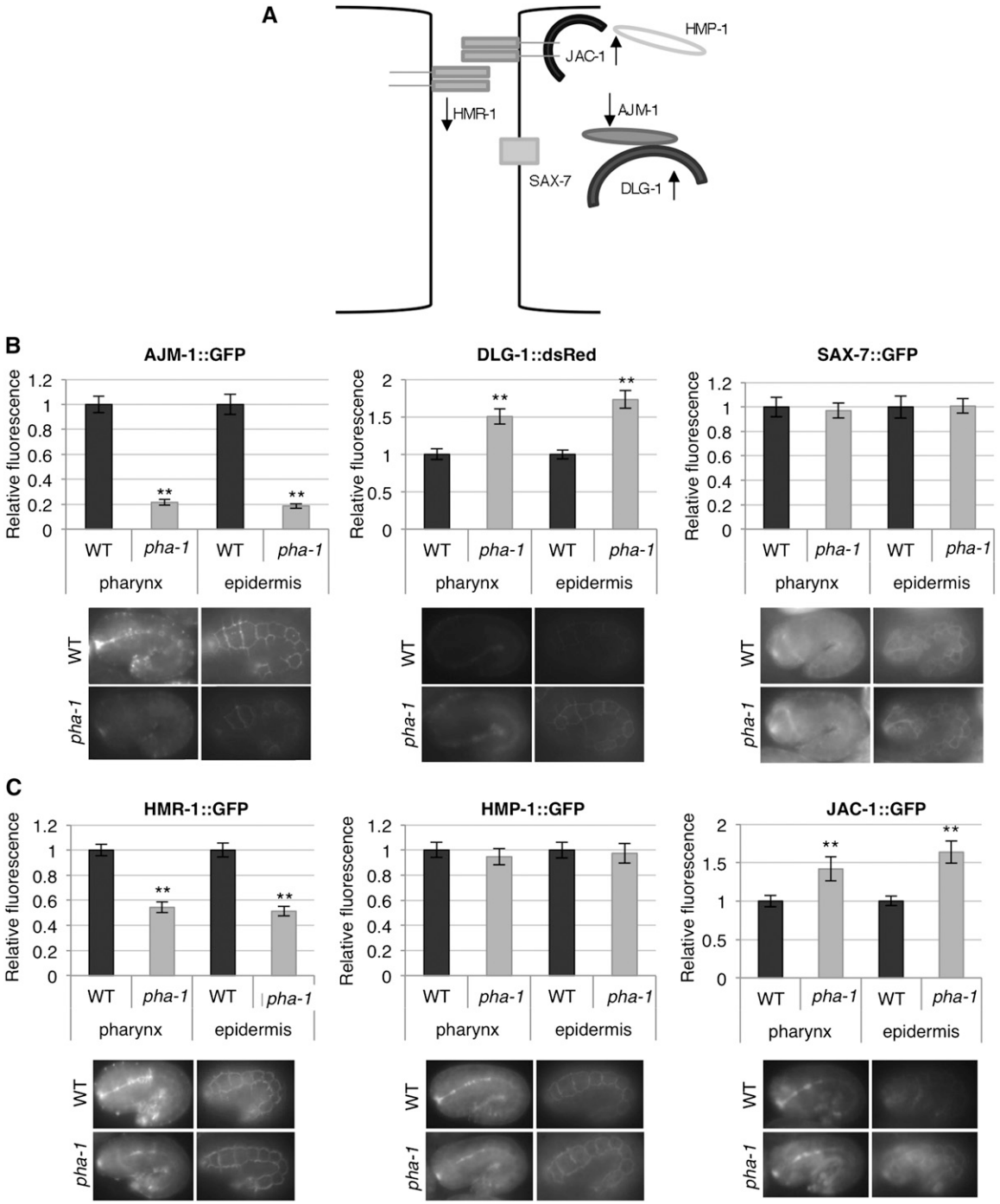

Figure 3 Loss of PHA-1 affects normal expression of epithelial junction markers. (A) Schematic representation of the proposed organization of epithelial junctions in *C. elegans*. Arrows show the direction of expression changes in the *pha-1(0)* background. (B and C) Quantification of fluorescence intensities of members of the DLG-1/AJM-1 complex (B) and cadherin–catenin complex (C) in wild-type and *pha-1(0)* mutant backgrounds. Also shown are representative fluorescence images of 1.5-fold-stage embryos. Fluorescence is expressed relative to wild type, which was arbitrarily set to 1.0. Error bars indicate 95% confidence intervals. Statistical analysis was performed using Student's *t*-test; $^{**}P < 0.001$.

or lost during development. On the basis of the phenotype of individual worms and the inheritance profile of the array, it was possible to infer tissue-specific requirements for *pha-1* and to correlate losses within particular lineages with specific phenotypes. A schematic summary of the mosaic analysis is shown in Figure 4A.

Intriguingly, in view of previous reports suggesting a role for PHA-1 in pharyngeal cell specification and differentiation, our data strongly indicate that PHA-1 was not required autonomously for the specification, differentiation, or function of most pharyngeal cells. Evidence includes our isolation of three adult animals in which *pha-1(+)* was missing

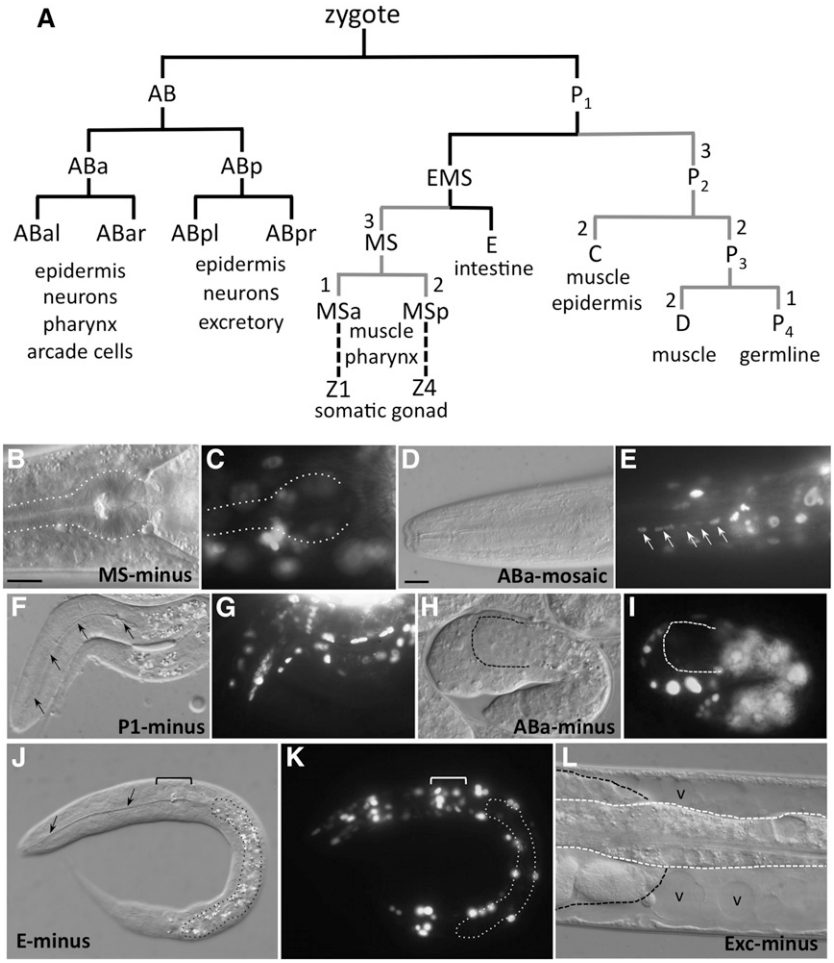

Figure 4 *pha-1(0)* mosaic analysis. (A) Early embryonic lineages are indicated along with major cell types produced by each lineage. Solid lines indicate lineages where *pha-1* plays an essential function. Numbers indicate viable L4 larvae or adults that were isolated with losses at the indicated cell divisions. (B–K) DIC, showing B, D, F, H, and J and corresponding fluorescence C, E, G, I, and K images of *pha-1(0)* mosaic animals carrying the *fdEx182* extrachromosomal array, which expresses both wild type *pha-1* and the SUR-5::GFP marker. Anterior is to the left. (B and C) L4-stage larva in which *pha-1* is absent from the MS lineage. Note the normal appearance of the posterior pharyngeal bulb and isthmus (dashed outline) despite the absence of *pha-1* activity. (D and E) Adult ABa-mosaic animal with a normal pharynx in which *pha-1* is present only in the left ventral tripartite epidermal section (pm2, e1, e2; indicated by arrows in E) derived from ABal. (F and G) P1-minus arrested L1 larva. Note the presence of a normal-appearing pharynx; solid arrows indicate the pharyngeal lumen in F. Also note normal body morphology. (H and I) Embryo (1.5-fold stage) that is missing *pha-1* in all cells derived from ABa. Dashed line indicates the boundary of the pharynx. Note the absence of any anterior pharyngeal extension. (J and K) Arrested L1 larvae in which *pha-1* is missing within the E lineage. Solid arrows in J indicate pharyngeal lumen; bracket in J, posterior bulb of pharynx (MS-plus); dashed line encircles the intestine (GFP-minus). (L) A clear (Clr) fluid-filled adult containing multiple vacuoles (v) that was missing *pha-1* in the excretory cell. The solid and open dashed lines denote the outlines of the intestine and gonad, respectively. Bar in B, 10 μm (for B, C, F–K) and bar in D, 10 μm (for D, E, and L).

entirely from the MS lineage (*i.e.*, MS-minus), as well as three animals in which *pha-1(+)* was missing in one of the daughters of MS (MSa/p). These MS-mosaic animals developed at normal rates and had pharynxes with wild-type morphology (Figure 4, B and C). Given that about half of the cells comprising the pharynx are derived from MS (Sulston *et al.* 1983), it appears that PHA-1 is dispensable for the normal development and function of at least half of the cells of this organ. Furthermore, although we failed to isolate adults in which *pha-1* was missing entirely from ABa or its daughters ABal and ABar, we did identify adults that had suffered multiple losses within the ABa sublineages that give rise to the pharynx. This included an adult in which only the left ventral tripartite epidermal section (pm2, e1, and e2, which are derived from ABal and ABar) retained the array within the ABa-derived pharyngeal lineage (Figure 4, D and E). Taken together, these findings suggest that PHA-1 does not function autonomously to promote the differentiation, morphogenesis, or function of the large majority of pharyngeal cells.

To complement the above analysis, we also analyzed embryos and arrested L1 larvae that were mosaic for *pha-1*. We identified seven P1-minus mosaics, which uniformly arrested as L1 larvae but contained pharynxes with relatively normal morphology (Figure 4, F and G). We also observed one L1 in which *pha-1* was missing within both the MS and ABar lineages. Although arrested, this animal had a pharynx with relatively normal morphology (data not shown). Given that the anteriormost pharyngeal epidermal cells, e1D, e1VL, and e1VR, are all derived from ABar, this would suggest that *pha-1* is not required in the e1 lineage for normal morphogenesis. (For pharyngeal anatomy, D signifies dorsal, whereas VL VR, and DL indicate ventral left, ventral right and dorsal left respectively; ant and post indicate anterior and posterior.) It also suggests that arcade cells derived from ABal (post-VL, post-DL, ant-DL, and ant-V) could be a focus for *pha-1*. Additional arrested L1s with little or no detectable expression in ABa-derived pharyngeal lineages were also observed, although the patterns of array inheritance within these animals were often quite complex. Nevertheless, such animals typically contained elongated pharynxes with relatively normal morphologies, suggesting that *pha-1* is not required within most ABa-derived pharyngeal cells for pharyngeal differentiation or morphogenesis. We also identified one ABa-minus ABp-plus embryo in which pharyngeal cell reorientation had failed (Figure 4, H and I). This finding suggested that although *pha-1* may not be autonomously required within most pharyngeal cells, there is

nevertheless a requirement for *pha-1* within the ABa lineage for pharyngeal morphogenesis to occur. Taken together, these findings suggest a requirement for PHA-1 within a subset of arcade cells, but because one or more pharyngeal epithelial cells is always close to one or more arcade cells in the ABa part of the cell lineage (Sulston *et al.* 1983), the possibility has not been excluded that PHA-1 acts within a subset of the ABa-derived pharyngeal cells (*e.g.*, e2) or that PHA-1 may be required in some combination of arcade and anterior pharyngeal cells. In addition, it is possible that PHA-1 also acts in other cells that are close to the pharyngeal epithelium and arcade cells in the cell lineage, such as the marginal cells.

PHA-1 performs essential functions in tissues outside of the pharynx

Interestingly, our mosaic analysis with the null allele also revealed several previously unknown tissue requirements for PHA-1. Most notably, we failed to observe viable larvae or adults in which *pha-1* was missing entirely from the intestinal lineage ($n > 10{,}000$). Rather, our data indicate that the absence of *pha-1* within the intestine leads to L1 larval arrest. Consistent with this, we identified 19 arrested L1 larvae in which the *pha-1*-rescuing array was lost in either the P1 (5), EMS (7), or E (7) lineages (Figure 4, J and K). These animals failed to display gross morphological defects of their intestines, and their intestinal cells appeared to contain microvilli (data not shown). Nevertheless, it is possible that these intestines contained subtle structural defects that we did not detect. It is also possible that these larvae arrested for reasons unrelated to intestinal defects, although their gross morphologies, including the pharynx, appeared normal (Figure 4, F and J). Moreover, the complete absence of viable intestine-minus mosaics strongly indicates that PHA-1 is required in this tissue. Somewhat surprisingly, we identified several adults that were missing *pha-1* in the majority of intestinal cells but were nevertheless viable. This included one sick, slow-growing adult that contained only four PHA-1-positive posterior gut nuclei (out of a total of 20 binucleate intestinal cells in the adult). Taken together, our data suggest that *pha-1* is autonomously required for some aspect of intestinal cell function but that this activity is not strictly required in all intestinal cells for growth and development to proceed.

We also observed a small percentage of mosaic animals (~1%) that became clear, vacuolated, and filled with fluid (the Clr phenotype), a defect associated with abnormal osmotic regulation (Nelson and Riddle 1984). The Clr phenotype did not become evident until ~2–3 days into adulthood, at which time clear fluid-filled animals containing multiple vacuoles could be detected (Figure 4L). Osmotic regulation in *C. elegans* is controlled by four cells that comprise the excretory system, a primitive analog of the renal system of vertebrates (Nelson *et al.* 1983). We examined the excretory system for the presence of the *pha-1* array in Clr adults. Notably, 21 of 24 Clr adults lacked detectable GFP expression in the excretory cell (one of four cells within the excretory system). In contrast, array expression in the excretory cell was detected in 25 of 25 adults that did not show the Clr phenotype. Furthermore, in the three Clr adults that showed GFP expression in the excretory cell, expression was not detected in the anatomically and lineally connected excretory duct cell. Taken together, our observations suggested a role for PHA-1 in the excretory system, in particular the excretory cell. We note, however, that correlating GFP expression with specific excretory cells using DIC optics was difficult, and the poor cellular morphology of the Clr adults further compounded this problem. Moreover, given the relatively late onset of the Clr phenotype, the role of PHA-1 in the excretory system may be subtle.

Although, as noted above, MS-minus animals grew normally to become viable adults, abnormal-looking proximal gonads were often observed, especially in older adult hermaphrodites. Specifically, PHA-1 appears to promote normal spermatogenesis, ovulation, or both. This is notable because MS gives rise to both Z1 (through MSp) and Z4 (through MSa), which produce the large majority of anterior and posterior somatic gonad cells, respectively (Figure 4A). Gonadal defects correlated with the reduction or absence of PHA-1 expression within individual gonad arms; MSa-minus/MSp-plus ($Z1^{+}/Z4^{-}$) mosaics showed defects specifically in the posterior gonad, whereas MSa-plus/MSp-minus ($Z1^{-}/Z4^{+}$) mosaics showed defects in the anterior gonad (Figure 5, A–D). Gonad arms deficient for *pha-1* produced endomitotic oocytes (Figure 5, C and D), which arise under conditions where oocytes fail to undergo timely fertilization (McCarter *et al.* 1997, 1999). We further identified 12 animals that were missing *pha-1* within sublineages of MS that give rise to the sheath and spermathecal cells of the somatic gonad (SS lineage). Although the patterns of array inheritance in these animals were often complex, we observed a clear correlation between the absence of *pha-1* expression within somatic gonad arms and the incidence of fertilization defects (Figure 5, E–J). This led to a reduction in the number of sperm and to the abnormal persistence of residual bodies, which are anucleate byproducts of spermatogenesis (L'Hernault 2006). In addition, MS-minus animals often contained abnormal embryos, oocytes, or oocyte fragments within the uterus (Figure 5K). Consistent with these data, MS-mosaic animals had reduced fecundity. Whereas nonmosaic controls had an average brood size of 264 (SD = 15.1; $n = 3$), animals that contained one positive and one negative gonad arm had an average brood size of 144 (SD = 34.4, $n = 4$). Nevertheless the complete absence of PHA-1 in the MS lineage did not preclude the production of progeny as we observed a single MS-minus animal with a brood size of 201. Collectively, these findings indicate an autonomous role for PHA-1 in the somatic gonad. In contrast, we found no essential role for PHA-1 within the developing germline (Figure 4). F_1 progeny from germline-minus adults were, as expected, embryonic lethal, and displayed a phenotype identical to that of *pha-1(0)* animals that failed to inherit the *pha-1(+)* array in the parental strain (data not shown).

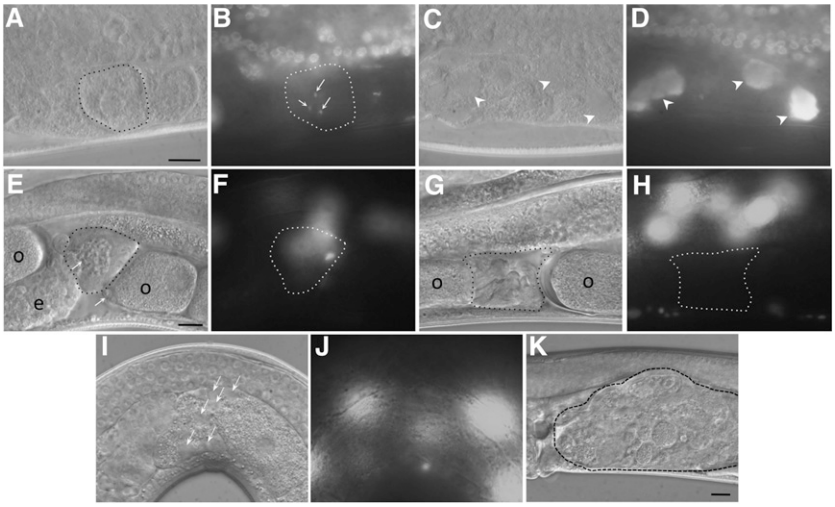

Figure 5 Gonadal defects in *pha-1* mosaic adults. (A–D) DIC and corresponding Hoechst staining of proximal gonad arms in an animal that is Z4-plus and Z1-minus for PHA-1. Z1 and Z4 give rise to the large majority of anterior and posterior somatic gonad cells, respectively. (A and B) Posterior gonad arm (*pha-1*-plus) with normal-appearing chromosomes (arrows) within the proximalmost oocyte (dashed line). (C and D) Anterior gonad arm (*pha-1*-minus) containing endomitotic oocytes. Arrowheads indicate swollen polyploid nuclei. Although not shown, more distal oocytes in the anterior gonad had normal nuclear morphologies. (E–H) DIC and corresponding GFP-fluorescence images from an adult with partial transmission of the *pha-1*-rescuing array within the MS lineage. o, oocytes; e, embryos. The proximal portion of each gonad is to the left. (E and F) Anterior gonad arm that contains normal-appearing sperm (arrows in E) within a *pha-1*-plus spermatheca (dashed line). (G and H) Posterior gonad arm that appears devoid of sperm within a *pha-1*-minus spermatheca (dashed line). (I and J) DIC and corresponding GFP-fluorescence image of the anterior proximal gonad region in an MS-minus *pha-1* mosaic adult. The proximal region of the gonad arm is to the left. Note the presence of spermatocyte residual bodies (arrows in I) in the region of the spermatheca. (K). DIC image of a uterus within an MS-minus *pha-1* mosaic showing abnormal oocytes or oocyte fragments that have been ovulated. Bar in A, 10 μm (for A–D); bar in D, 10 μm (for D–J); bar in K, 10 μm.

Additional phenotypes observed in *pha-1* mosaic animals included irregularly shaped (Lpy) and short and fat (Dpy) larvae and adults. The Lpy/Dpy phenotypes are consistent with previously described roles for PHA-1 during embryonic morphogenesis (Schnabel and Schnabel 1990; Granato *et al.* 1994a; Fay *et al.* 2004). Though difficult to study using classical mosaic analysis, Lpy/Dpy animals could be expected to arise when the array is absent within particular regions of the epidermis or possibly when the copy number of the array within the hypodermal syncytium is strongly reduced. Notably, loss of the array within either the ABa or ABp lineages, which are the major contributors to the epidermis, was never detected in hatched larvae (Figure 4). In contrast, loss within the C lineage, which contributes to the epidermis but to a lesser extent than ABa or ABp, was detected in morphologically normal viable adults (Figure 4). Finally, we occasionally observed adult hermaphrodites that retained abnormal numbers of eggs (Egl; data not shown). Although bloated, these Egl animals had vulvae that appeared normal and were able to lay eggs. Therefore, PHA-1 may play a minor role in some aspect of vulval development or in the neurons or muscles that are required for rhythmic egg laying.

Discussion

The role of PHA-1 in *C. elegans* development has been difficult to assess, given the previous lack of an available null mutation, the absence of any conserved functional domains, the broad pattern of cytoplasmic expression, and the somewhat contradictory nature of published reports. Here we demonstrate that PHA-1 does not have an autonomous role in the differentiation, morphogenesis, or function of most or all pharyngeal cells (Figure 4). Rather, the role of PHA-1 in pharyngeal morphogenesis may reflect a requirement within a subset of arcade cells, a subset of pharyngeal epithelial cells, or both (Figure 1). At this time it is not feasible to distinguish between these possibilities because promoters are not available for expressing *pha-1* specifically within either the arcade or anterior pharyngeal epithelial cells in early embryos. Furthermore, there may be some plasticity in the requirement for PHA-1 within arcade and/or pharyngeal epithelial cell types as opposed to an absolute requirement within any single cell type. Our general findings for PHA-1 contrast with published reports for the transcriptional regulator PHA-4/FOXO, which directly regulates the differentiation of all pharyngeal cell types (Mango *et al.* 1994; Horner *et al.* 1998; Gaudet and Mango 2002; Mango 2009).

Our mosaic analysis of the *pha-1(0)* mutant also implicates several new functions for PHA-1, including roles in the intestine, somatic gonad, and excretory system (Figure 4). Notably, these defects are not observed in homozygous *pha-1(ts)* strains shifted to the nonpermissive temperature after embryogenesis (Schnabel and Schnabel 1990; Granato *et al.* 1994a) (data not shown). How defects in these distinct tissues might be connected to a single cellular or molecular function is currently unclear. However, the ability of mutations in *sup-35*, *sup-36*, and *sup-37* to suppress all of the *pha-1*-associated defects uncovered by our mosaic analysis suggests that a common underlying molecular mechanism may account for the phenotype of different tissues. This is also consistent with a mosaic analysis demonstrating a role for SUP-37 in both the somatic gonad and intestine (Fay *et al.* 2012), two tissues implicated in our mosaic analysis of *pha-1*. More generally, we can conclude that the functional interactions of SUP-35–37 with PHA-1 are not limited to those associated with foregut morphogenesis.

We also show that PHA-1 is required in AB-derived lineages, which contribute to the large majority of the epidermis,

for normal morphogenesis. This is consistent with morphological abnormalities observed in *pha-1* mutant embryos and larvae. Moreover, the role of PHA-1 in the epidermis is supported by our analysis of apical junction markers in the epithelium of *pha-1(0)* mutants (Figure 2 and Figure 3). Namely, expression levels of AJM-1 and HMR-1/cadherin were reduced, whereas levels of DLG-1/discs large and JAC-1/p120-catenin were elevated. Although the precise meaning behind the specific pattern of apical marker deregulation in *pha-1(0)* mutants is unclear, these changes clearly implicate PHA-1 in the normal function of the epithelium, possibly by regulating cell polarity, differentiation, or epithelial junctions. We note that although the strongly reduced expression of AJM-1 may account, at least in part, for the body morphogenesis defects observed in *pha-1* mutants (Schnabel and Schnabel 1990; Granato *et al.* 1994a; Fay *et al.* 2004), it cannot explain defects in pharyngeal development, as *ajm-1(ok160)* null mutants did not display defects in pharyngeal morphogenesis (data not shown). Interestingly, a reduction in *hmr-1* levels by RNAi has been reported to result in a Pun phenotype (Ferrier *et al.* 2011), consistent with the possibility that the unattached pharynx in *pha-1* mutants is related to reduced HMR-1 levels. We also raise the possibility that initial attachment of the pharynx and the ensuing biomechanical tension experienced by pharyngeal cells may in part promote pharyngeal cell differentiation as has been shown for various cell types in other systems (Benjamin and Hillen 2003; Mammoto *et al.* 2012; Franze 2013; Janmey *et al.* 2013). Whether this phenomenon occurs in *C. elegans*, however, is unknown.

PHA-1 family members have expanded and rapidly evolved within the *elegans* and *Japonica* super groups. Our findings suggest that PHA-1 family members may regulate numerous aspects of nematode development in these species. It is worth noting that one of our identified downstream targets of PHA-1, the apical junction protein AJM-1, is also not well conserved outside of the nematode phylum. Thus, *pha-1* and *sup-35–37* may represent a regulatory module that has coevolved with *ajm-1* within the *Caenorhabditis* lineage.

Acknowledgments

We thank Amy Fluet for editing, Anna Justis for technical help, and the National BioResource Project of Japan for providing strains. This work was supported by grant GM066868 from the National Institutes of Health (NIH). A.K. was supported in part by the Wyoming IDeA Networks for Biomedical Research Excellence (INBRE) Program from the NIH (P20 GM103432). Some strains were provided by the *Caenorhabditis* Genetics Center, which is funded by NIH Office of Research Infrastructure Programs (P40 OD010440).

Literature Cited

Achilleos, A., A. M. Wehman, and J. Nance, 2010 PAR-3 mediates the initial clustering and apical localization of junction and polarity proteins during C. elegans intestinal epithelial cell polarization. Development 137: 1833–1842.

Albertson, D. G., and J. N. Thomson, 1976 The pharynx of Caenorhabditis elegans. Philos. Trans. R. Soc. Lond. B Biol. Sci. 275: 299–325.

Benjamin, M., and B. Hillen, 2003 Mechanical influences on cells, tissues and organs: 'Mechanical Morphogenesis'. Eur. J. Morphol. 41: 3–7.

Chen, L., B. Ong, and V. Bennett, 2001 LAD-1, the Caenorhabditis elegans L1CAM homologue, participates in embryonic and gonadal morphogenesis and is a substrate for fibroblast growth factor receptor pathway-dependent phosphotyrosine-based signaling. J. Cell Biol. 154: 841–855.

Fay, D. S., E. Large, M. Han, and M. Darland, 2003 lin-35/Rb and ubc-18, an E2 ubiquitin-conjugating enzyme, function redundantly to control pharyngeal morphogenesis in C. elegans. Development 130: 3319–3330.

Fay, D. S., X. Qiu, E. Large, C. P. Smith, S. Mango *et al.*, 2004 The coordinate regulation of pharyngeal development in C. elegans by lin-35/Rb, pha-1, and ubc-18. Dev. Biol. 271: 11–25.

Fay, D. S., S. R. Polley, J. Kuang, A. Kuzmanov, J. W. Hazel *et al.*, 2012 A regulatory module controlling pharyngeal development and function in Caenorhabditis elegans. Genetics 191: 827–843.

Ferrier, A., A. Charron, Y. Sadozai, L. Switaj, A. Szutenbach *et al.*, 2011 Multiple phenotypes resulting from a mutagenesis screen for pharynx muscle mutations in Caenorhabditis elegans. PLoS ONE 6: e26594.

Franze, K., 2013 The mechanical control of nervous system development. Development 140: 3069–3077.

Gaudet, J., and S. E. Mango, 2002 Regulation of organogenesis by the Caenorhabditis elegans FoxA protein PHA-4. Science 295: 821–825.

Granato, M., H. Schnabel, and R. Schnabel, 1994a Genesis of an organ: molecular analysis of the pha-1 gene. Development 120: 3005–3017.

Granato, M., H. Schnabel, and R. Schnabel, 1994b pha-1, a selectable marker for gene transfer in C. elegans. Nucleic Acids Res. 22: 1762–1763.

Horner, M. A., S. Quintin, M. E. Domeier, J. Kimble, M. Labouesse *et al.*, 1998 pha-4, an HNF-3 homolog, specifies pharyngeal organ identity in Caenorhabditis elegans. Genes Dev. 12: 1947–1952.

Janmey, P. A., R. G. Wells, R. K. Assoian, and C. A. McCulloch, 2013 From tissue mechanics to transcription factors. Differentiation 86: 112–120.

Kemphues, K., 2005 Essential genes. WormBook pp. 1–7.

Koppen, M., J. S. Simske, P. A. Sims, B. L. Firestein, D. H. Hall *et al.*, 2001 Cooperative regulation of AJM-1 controls junctional integrity in Caenorhabditis elegans epithelia. Nat. Cell Biol. 3: 983–991.

L'Hernault, S. W., 2006 Spermatogenesis. WormBook pp. 1–14, http://www.wormbook.org/chapters/www_spermatogenesis/spermatogenesis.html.

Labouesse, M., 2006 Epithelial junctions and attachments. WormBook pp. 1–21.

Lynch, A. M., and J. Hardin, 2009 The assembly and maintenance of epithelial junctions in C. elegans. Front. Biosci. 14: 1414–1432 (Landmark Ed).

Mammoto, A., T. Mammoto, and D. E. Ingber, 2012 Mechanosensitive mechanisms in transcriptional regulation. J. Cell Sci. 125: 3061–3073.

Mango, S. E., 2007 The C. elegans pharynx: a model for organogenesis. WormBook pp. 1–26.

Mango, S. E., 2009 The molecular basis of organ formation: insights from the C. elegans foregut. Annu. Rev. Cell Dev. Biol. 25: 597–628.

Mango, S. E., E. J. Lambie, and J. Kimble, 1994 The pha-4 gene is required to generate the pharyngeal primordium of Caenorhabditis elegans. Development 120: 3019–3031.
Mani, K., and D. S. Fay, 2009 A mechanistic basis for the coordinated regulation of pharyngeal morphogenesis in Caenorhabditis elegans by LIN-35/Rb and UBC-18-ARI-1. PLoS Genet. 5: e1000510.
McCarter, J., B. Bartlett, T. Dang, and T. Schedl, 1997 Soma-germ cell interactions in Caenorhabditis elegans: multiple events of hermaphrodite germline development require the somatic sheath and spermathecal lineages. Dev. Biol. 181: 121–143.
McCarter, J., B. Bartlett, T. Dang, and T. Schedl, 1999 On the control of oocyte meiotic maturation and ovulation in Caenorhabditis elegans. Dev. Biol. 205: 111–128.
McMahon, L., R. Legouis, J. L. Vonesch, and M. Labouesse, 2001 Assembly of C. elegans apical junctions involves positioning and compaction by LET-413 and protein aggregation by the MAGUK protein DLG-1. J. Cell Sci. 114: 2265–2277.
Nelson, F. K., P. S. Albert, and D. L. Riddle, 1983 Fine structure of the Caenorhabditis elegans secretory-excretory system. J. Ultrastruct. Res. 82: 156–171.
Nelson, F. K., and D. L. Riddle, 1984 Functional study of the Caenorhabditis elegans secretory-excretory system using laser microsurgery. J. Exp. Zool. 231: 45–56.
Okkema, P. G., E. Ha, C. Haun, W. Chen, and A. Fire, 1997 The Caenorhabditis elegans NK-2 homeobox gene ceh-22 activates pharyngeal muscle gene expression in combination with pha-1 and is required for normal pharyngeal development. Development 124: 3965–3973.
Pettitt, J., E. A. Cox, I. D. Broadbent, A. Flett, and J. Hardin, 2003 The Caenorhabditis elegans p120 catenin homologue, JAC-1, modulates cadherin-catenin function during epidermal morphogenesis. J. Cell Biol. 162: 15–22.
Polley, S. R., A. Kuzmanov, J. Kuang, J. Karpel, V. Lazetic *et al.*, 2014 Implicating SCF complexes in organogenesis in Caenorhabditis elegans. Genetics 196: 211–223.
Portereiko, M. F., and S. E. Mango, 2001 Early morphogenesis of the Caenorhabditis elegans pharynx. Dev. Biol. 233: 482–494.
Qiu, X., and D. S. Fay, 2006 ARI-1, an RBR family ubiquitin-ligase, functions with UBC-18 to regulate pharyngeal development in C. elegans. Dev. Biol. 291: 239–252.
Raich, W. B., C. Agbunag, and J. Hardin, 1999 Rapid epithelial-sheet sealing in the Caenorhabditis elegans embryo requires cadherin-dependent filopodial priming. Curr. Biol. 9: 1139–1146.
Sarov, M., J. I. Murray, K. Schanze, A. Pozniakovski, W. Niu *et al.*, 2012 A genome-scale resource for in vivo tag-based protein function exploration in C. elegans. Cell 150: 855–866.
Schnabel, H., and R. Schnabel, 1990 An organ-specific differentiation gene, pha-1, from Caenorhabditis elegans. Science 250: 686–688.
Schnabel, H., G. Bauer, and R. Schnabel, 1991 Suppressors of the organ-specific differentiation gene pha-1 of *Caenorhabditis elegans*. Genetics 129: 69–77.
Shaw, W. R., J. Armisen, N. J. Lehrbach, and E. A. Miska, 2010 The conserved miR-51 microRNA family is redundantly required for embryonic development and pharynx attachment in *Caenorhabditis elegans*. Genetics 185: 897–905.
Stiernagle, T., 2006 Maintenance of C. elegans. WormBook pp. 1–11.
Sulston, J. E., E. Schierenberg, J. G. White, and J. N. Thomson, 1983 The embryonic cell lineage of the nematode Caenorhabditis elegans. Dev. Biol. 100: 64–119.
Yochem, J., T. Gu, and M. Han, 1998 A new marker for mosaic analysis in *Caenorhabditis elegans* indicates a fusion between hyp6 and hyp7, two major components of the hypodermis. Genetics 149: 1323–1334.
Yochem, J., M. Sundaram, and E. A. Bucher, 2000 Mosaic analysis in Caenorhabditis elegans. Methods Mol. Biol. 135: 447–462.
Yochem, J. K., 2006 Nomarski images for learning the anatomy, with tips for mosaic analysis. WormBook pp. 1–47.

Communicating editor: D. Greenstein

GENETICS

Supporting Information
http://www.genetics.org/lookup/suppl/doi:10.1534/genetics.114.166876/-/DC1

Analysis of PHA-1 Reveals a Limited Role in Pharyngeal Development and Novel Functions in Other Tissues

Aleksandra Kuzmanov, John Yochem, and David S. Fay

DOI: 10.1534/genetics.114.166876

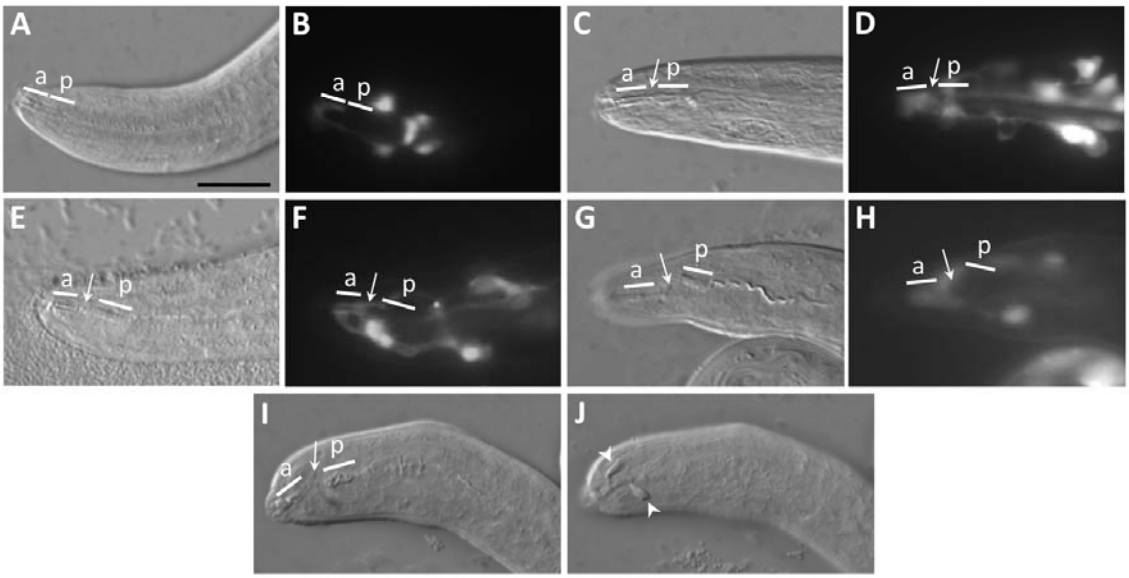

Figure S1 The *pha-1(ts)* mutant shows defects in the arcade–pharynx junction. (A–H) DIC (A,C,E,G) and corresponding fluorescence (B,D,F,H) images of wild-type (A,B) and *pha-1(ts)* mutant larvae (C–H) expressing the *bath-15*::GFP arcade cell reporter, which marks the anterior half of the buccal capsule. Anterior is to the left. Arcade (a) and pharyngeal (p) contributions to the buccal capsule (white lines) are indicated. Arrow indicates region of separation or aberrant morphology at the division between the arcade- and pharynx-derived buccal capsule. The *bath-15*::GFP reporter marks both the cell bodies (posterior and round) and processes (anterior and posterior, variably shaped) of the arcade cells. Note that the anterior portion of the buccal capsule in mutant animals where the capsule has been severed coincides with the location of anterior *bath-15* expression, consistent with breakage occurring at the junction of the arcade and epithelial cells. (I,J) *pha-1(ts)* larva with a severed buccal capsule (I) and abnormal arcade cell morphology (J), as indicated by arrowheads. I and J depict different focal plains of the same larva. Size bar in A represents 10 μm for A–J.

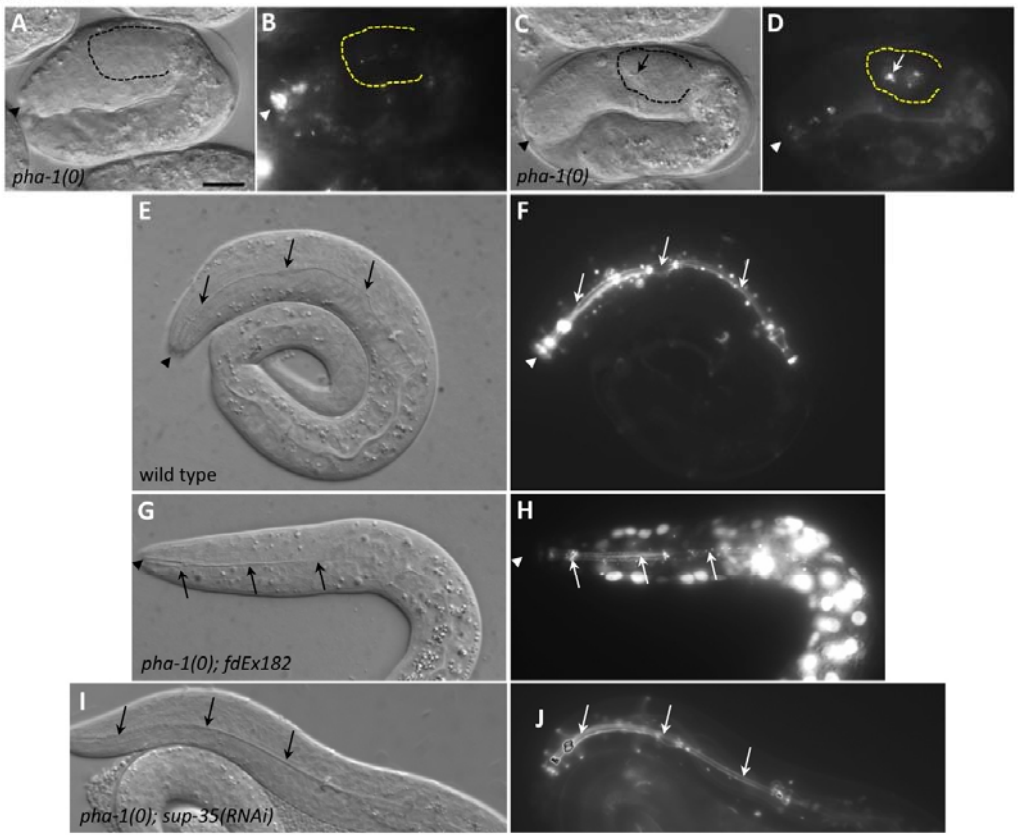

Figure S2 AJM-1::GFP expression in various strain backgrounds. (A–J) DIC (A,C,E,G, I) and corresponding AJM-1::GFP fluorescence (B,D,F,H,J) images. Anterior is to the left, with genotypes indicated within panels. Arrows indicate pharyngeal lumen. Note that expression of AJM-1::GFP in terminally arrested *pha-1(0)* embryos (A–D) is weaker and disorganized as compared with a recently hatched wild-type L1 larva of similar chronological age (E,F). In addition, AJM-1::GFP expression is largely missing in the region between the non-elongated pharynx (dashed yellow line, A–D) and the developing buccal cavity (arrowhead). (G,H) Expression of AJM-1::GFP in a *pha-1(0)* L1 larva that has been rescued by wild-type *pha-1* genomic sequences present on an extrachromosomal array (*fdEx182)*. Additional fluorescence in nuclei in panel H is due to the expression of SUR-5::GFP by the *fdEx182* array. (I,J) AJM-1::GFP expression is restored in *pha-1(0)* mutants suppressed by *sup-35(RNAi)*. Size bar in A represents 10 µm for A–J.